A Generalized Virtual Energy Storage Model for V2G Charging and Discharging Flexibility Characterization, Aggregation and Forecasting

Boning Zhao, Yu Yang, *Member, IEEE,* Qing-Shan Jia, *Senior Member, IEEE,* Yiqun Yang, and Xiaohong Guan, *Life Fellow, IEEE*

***Abstract*—The rapid proliferation of electric vehicles (EVs), together with the emerging vehicle-to-grid (V2G) technologies, introduces substantial operational flexibility to modern power systems. However, effectively leveraging such flexibility faces challenges of aggregating the small-scale and heterogeneous operational flexibility of vehicles under stochastic driving behaviors. To address these challenges, this paper proposes a generalized virtual energy storage (VES) model to characterize the operational flexibility for both uni-directional EVs and bi-directional V2Gs. *First*, the VES model enables computationally efficient aggregation of heterogeneous vehicle flexibility while preserving the essential operational constraints. *Second*, a structured integration approach is developed to reduce the dimensionality of VES model parameters and eliminate the need to explicitly predict the energy variation terms induced by stochastic vehicle arrivals and departures. *Third*, a physics-constrained forecasting approach is proposed to ensure coherent and physically consistent predictions of the multi-dimensional VES model parameters. The proposed framework is validated using real-world charging datasets and applied to joint energy and frequency market participation of charging station. The results show that the proposed methods achieve a multi-time-scale day-ahead modeling accuracy of aggregated vehicle flexibility at approximately 86% with a Pearson correlation coefficient (CORR) of 0.93. For joint market participation, the market performance gap induced by aggregation remains below 5%, while the combined loss caused by aggregation and prediction is within 10%. Notably, the computational efficiency of obtaining optimal bidding strategies is improved from 10–22 mins to seconds through aggregation.**

***Index Terms*—Vehicle-to-grid (V2G), charging and discharging flexibility, virtual energy storage (VES) model, physics-constrained forecasting method, energy and frequency market**

I. Introduction

DRIVEN by the decarbonization and electrification of transportation sector, electric vehicles (EVs) have experienced rapid adoption around the world. As of 2024, global electric cars had reached 58 million, accounting for 4% of total passenger car fleet. The annual sales of electric cars have been growing at an exponential rate worldwide. As a center of growth, nearly half of China's car sales were electric in 2024 [1]. Many countries even announced plans to phase out internal combustion engine (ICE) passenger cars, such as United Kingdom, France, and Norway [2]. The rising adoption of EVs in place of fossil-fueled vehicles brings both challenges and opportunities to modern power system operation. On one hand, the incurred substantial charging demand represents a rapidly growing stochastic electric load, exacerbating the stress of power grid operation [3]. On the other hand, EVs represent substantial flexible resources that can be exploited for supporting modern power system operation. While the charging demand can be shifted across time due to their long parking duration, the emerging vehicle-to-grid (V2G) technologies meanwhile enable connected vehicles to operate as distributed energy storage systems. However, unlocking such flexibility relies on models to aggregate the small-scale, heterogeneous, stochastic and temporally coupled flexibility of individual vehicles to enable system-level commitment and dispatch when providing grid services, such as demand response [4], peak shaving [5], frequency regulation [6], etc.

In recent years, many works have focused on developing methods to characterize and aggregate of charging and discharging flexibility of EVs. Typically, Pertl et al. [7] proposed to estimate the aggregated energy storage capacity of fleet by summing up the individual battery capacities of connected vehicles. Zhang et al. [8] and Yi et al. [9] proposed to characterize the aggregated charging flexibility of EVs by upper and lower energy and power boundaries, which provides an outer approximation of feasible charging regions. While the above methods are model-based and computationally efficient, another class is optimization-based and depends on comprehensive optimization to obtain the aggregated models. For example, Yan et al. [10] proposed to characterize the aggregated charging flexibility of EV fleet by upper and lower power boundaries obtained from solving the comprehensive EV charging scheduling problem. Particularly, this method converts time-coupled EV charging demand into time-independent power-flexible loads. Some other optimization-based methods investigated charging flexibility characterization and aggregation from a more mathematical perspective. Specifically, the charging flexibility of individual vehicles corresponds to their feasible charging regions considering their

This work is supported by the National Natural Science Foundation of China (62403373, 72595834, 62192752).

B. Zhao and Y. Yang are with School of Automation Science and Engineering, Xi'an Jiaotong University, Shaanxi, China (e-mail: zhaoboning@stu.xjtu.edu.cn, yangyu21@xjtu.edu.cn). *Y. Yang is the corresponding author.*

Q. -S. Jia is with the Center for Intelligent and Networked Systems, Department of Automation, BNRist, Tsinghua University, Beijing 100084, China (e-mail: jiaqs@tsinghua.edu.cn).

Y. Q. Yang is with the Department of Electrical and Computer Engineering, Duke University, Durham, NC 27708, USA (e-mail: yy495@duke.edu).

X. Guan is with the Ministry of Education Key Laboratory for Intelligent Networks and Network Security Laboratory, Xi'an Jiaotong University, Xi'an 710049, China, also with the Center for Intelligent and Networked Systems, Department of Automation, Tsinghua University, Beijing 100084, China (e-mail: xhguan@tsinghua.edu.cn).

charging requirement and charging rate limits, while flexibility aggregation corresponds to computing the Minkowski sum of those feasible regions. However, computing the Minkowski sum of heterogeneous and regular regions is NP-hard. As a result, many works investigated different means to overcome the computational challenge. Müller et al. [11] proposed to use optimization-based approach to inner approximate the polytopic feasible sets of individual vehicles using zonotopes which facilitate Minkowski sum calculation. Taha et al. [12] used a class of AH-polytopes to inner approximate the half-space representations of individual vehicle charging flexibility. Wen et al. [13] employed Fourier-Motzkin elimination method to calculate the Minkowski sum of the feasible operational regions of distributed energy resources (DERs), yielding a rigorous but computationally intensive solution. Slightly different, Taheri et al. [14] relied on data-driven approach to obtain the feasible polytope operational region of DERs. While those optimization-based approaches are theoretically rigorous, their high computation cost often represents a major obstacle for practical application. Existing model-based methods either provide only a coarse estimation or do not account for the departures of vehicles, failing to capture the actual energy available for grid services. Overall, there still lacks computationally efficient and effective aggregation methods that can support the wide range of energy services to be provided.

Another key issue of charging flexibility aggregation of EVs lies in the uncertainty arising from the random driving and parking behaviors. Aggregated models are often required for energy planning ahead of time, therefore how to deal with the uncertainty represents another major challenge. Therefore, some works focused on modeling the uncertain driving and parking behaviors using Markov chains [15] or Gaussian models [16] and relied on them to simulate the random behaviors of vehicles when aggregation. Another line of works proposed to construct probabilistic aggregated flexibility sets instead of deterministic ones to account for the uncertainty. For example, Zhang et al. [17] characterized the aggregated charging flexibility of EVs by a chance-constrained probabilistic polytope. Mukhi et al. [18] constructed robust aggregated flexibility sets for EV fleet with probabilistic guarantees. Another means to address uncertainty is through forecasting (see [7, 8, 19, 20] for examples). This class of works typically relies on forecasting methods to obtain aggregated charging flexibility for the future. As easy to implement, forecasting-based methods have been widely adopted. However, these works generally did not consider the coupling and coherence of multi-dimensional parameters associated with the aggregated models.

Given the research gaps discussed above, this paper studies the charging and discharging flexibility characterization, aggregation and forecasting of EVs and V2Gs under uncertainty. This paper uses V2Gs to indicate vehicles capable of bi-directional charging and discharging, and EVs to represent uni-directional charge-only vehicles when connected to smart chargers. **Our main contributions are as follows.**

- We propose a generalized virtual energy storage (VES) model that enables the operational flexibility characterization of bi-directional V2Gs and uni-directional EVs at both the vehicle and fleet levels. Particularly, the proposed models enable computationally efficient aggregation of the heterogeneous vehicle operational flexibility.
- We further propose a structured integration of the multi-dimensional parameters with the VES models. This can effectively reduce the dimensionality of model parameters and overcome the challenge of predicting the energy change terms caused by the random arrival and departure events of vehicles.
- We further propose a physics-constrained forecasting method for day-ahead aggregated vehicle operational flexibility predictions. Particularly, the method incorporates physics-constrained blocks to enable coherent and physically consistent predictions of the multi-dimensional VES model parameters, which are critical to ensure the feasibility of downstream optimization problems.

The effectiveness of proposed characterization, aggregation and forecasting method is evaluated using real-world charging dataset and validated for the joint energy and frequency market participation. Results show that the forecasting method enables multi-time-scale day-ahead predictions of aggregated vehicle flexibility at a prediction accuracy close to 86% and the Pearson Correlation Coefficient (CORR) close to 0.93. Particularly, the physics-constrained blocks are essential to ensure a coherent and physically consistent prediction of the multi-dimensional parameters of the VES models. For the joint market participation, results show that the performance loss induced by aggregation is below 5%, while the combined loss caused by both prediction and aggregation remains under 10%. Whereas the computational efficiency to obtain the optimal bidding strategies of charging stations is significantly improved from 10–22 minutes to second levels.

The remainder of this paper is as follows. Section II presents the charging and discharging flexibility characterization and aggregation for V2Gs and EVs. Section III introduces the physics-constrained charging and discharging flexibility prediction for vehicles at aggregated level. Section IV evaluates the proposed characterization, aggregation and forecasting methods, as well as its applications to support market participation of charging stations. Section V concludes this paper.

II. V2G Charging and Discharging Flexibility Characterization and Aggregation

This section focuses on bi-directional V2Gs and further discuss how the results can be extended to uni-directional EVs. The flexibility of individual V2Gs refers to their feasible charging and discharging regions considering their charging requirements and battery operating limits. Flexibility aggregation of a fleet corresponds to identifying the feasible region of aggregated charging and discharging trajectories accounting for the individual vehicles' charging requirements and battery operating limits. In terms of the flexibility characterization and aggregation of V2Gs, main notations to be visited are summarized in TABLE I.

A. Individual V2G Charging and Discharging Flexibility Characterization

Given the charging requirement, the feasible charging and discharging region of a V2G is bounded by two extreme cases:

TABLE I
MAIN NOTATIONS FOR V2G

Notation	Definition	Units
Ω^{V2G}	V2G fleet	–
$E_i^{\mathrm{V2G,cap}}$	Energy capacity of V2G i	kWh
$P_i^{\mathrm{V2G,ch/dis,max}}$	Power capacity of V2G i	kW
T	Entire scheduling window	–
Δt	Char/discharging scheduling interval	h
$t_i^{\mathrm{V2G,arr}}, t_i^{\mathrm{V2G,dep}}$	Arrival and departure time of V2G i	–
$E_i^{\mathrm{V2G,arr}}$	Energy level of V2G i upon arrival	kWh
$E_i^{\mathrm{V2G,dep}}$	Desirable energy level of V2G i at departure	kWh
$E_i^{\mathrm{V2G,req}}$	Required charging energy of V2G i	kWh
$\eta^{\mathrm{V2G,ch/dis}}$	Char/discharging efficiency of V2Gs	–
$P_{i,t}^{\mathrm{V2G,ch/dis}}$	Scheduled char/discharging power during time t	kW
$E_{i,t}^{\mathrm{V2G}}$	Energy level of V2G i at the end of time t	kWh

fastest charging where the V2G charges at its maximum rate upon arrival until its battery is full; **slowest charging** where the V2G discharges to the grid at maximum rate upon arrival until its battery is depleted or the minimum remaining time to fill its charging demand arrives.

Specifically, for an V2G i with parking duration $T_i^{\mathrm{V2G}} := [t_i^{\mathrm{V2G,arr}}, t_i^{\mathrm{V2G,dep}}]$ and desirable energy state at departure $E_i^{\mathrm{V2G,dep}} := E_i^{\mathrm{V2G,arr}} + E_i^{\mathrm{V2G,req}}$, the feasible charging and discharging trajectories are bounded by an upper and lower energy envelope $\{E_{i,t}^{\mathrm{V2G,max}}\}$ and $\{E_{i,t}^{\mathrm{V2G,min}}\}$ corresponding to the fastest and slowest charging trajectories as illustrated in Fig. 1. However, it should be emphasized that the energy envelopes alone are not sufficient to characterize the feasible charging and discharging region of the V2G. In addition to lying in between the upper and lower energy envelopes, a feasible charging and discharging trajectory should respect the vehicle's charging and discharging rate limits.

To account for the above aspects, we use the following model to characterize the charging and discharging flexibility of individual V2Gs:

$$0 \le P_{i,t}^{\mathrm{V2G,ch}} \le P_i^{\mathrm{V2G,ch,max}}, \qquad \forall t \in T_i^{\mathrm{V2G}} \tag{1a}$$

$$0 \le P_{i,t}^{\mathrm{V2G,dis}} \le P_i^{\mathrm{V2G,dis,max}}, \qquad \forall t \in T_i^{\mathrm{V2G}}. \tag{1b}$$

$$E_{i,t}^{\mathrm{V2G}} = \begin{cases} E_{i,t-1}^{\mathrm{V2G}} + E_i^{\mathrm{V2G,arr}}, & \forall t = t_i^{\mathrm{V2G,arr}}, \\ E_{i,t-1}^{\mathrm{V2G}} + \Delta E_{i,t}^{\mathrm{V2G}}, & \forall t_i^{\mathrm{V2G,arr}} < t \le t_i^{\mathrm{V2G,dep}}, \\ E_{i,t-1}^{\mathrm{V2G}} - E_i^{\mathrm{V2G,dep}}, & \forall t > t_i^{\mathrm{V2G,dep}}. \end{cases} \tag{1c}$$

$$\Delta E_{i,t}^{\mathrm{V2G}} = \big(P_{i,t}^{\mathrm{V2G,ch}} \eta^{\mathrm{V2G,ch}} - P_{i,t}^{\mathrm{V2G,dis}} / \eta^{\mathrm{V2G,dis}}\big)\Delta t, \forall t \in T_i^{\mathrm{V2G}}. \tag{1d}$$

$$E_{i,t}^{\mathrm{V2G,min}} \le E_{i,t}^{\mathrm{V2G}} \le E_{i,t}^{\mathrm{V2G,max}}, \quad \forall t \in T_i^{\mathrm{V2G}}. \tag{1e}$$

Cons. (1a)–(1b) enforce charging and discharging rate limits, while (1c)–(1d) describe the corresponding dynamics. The energy state is reset upon departure ($t > t_i^{\mathrm{V2G,dep}}$) to indicate disconnection. Cons. (1e) impose upper and lower energy envelopes that bound the charging and discharging trajectories. Compared with directly using battery capacity limits, these energy envelopes provide a tighter characterization of the feasible charging and discharging region of individual vehicles, which is critical for developing accurate flexibility aggregation models for V2G fleets.

The above model offers a tight representation of individual V2G flexibility. However, it is not additive across vehicles due to heterogeneous parking durations and therefore not suitable for aggregation. To address this issue, we introduce binary variables to indicate the connected and disconnected status of the V2G over the scheduling horizon T:

$$X_{i,t} = \begin{cases} 1, & \forall t \in [t_i^{\mathrm{V2G,arr}}, t_i^{\mathrm{V2G,dep}}] \\ 0, & \forall t \notin [t_i^{\mathrm{V2G,arr}}, t_i^{\mathrm{V2G,dep}}] \end{cases}$$

This enables us to transform model (1) into

$$0 \le P_{i,t}^{\mathrm{V2G,ch}} \le X_{i,t} \cdot P_i^{\mathrm{V2G,ch,max}}, \tag{2a}$$

$$0 \le P_{i,t}^{\mathrm{V2G,dis}} \le X_{i,t} \cdot P_i^{\mathrm{V2G,dis,max}}, \tag{2b}$$

$$E_{i,t}^{\mathrm{V2G}} = E_{i,t-1}^{\mathrm{V2G}} + (P_{i,t}^{\mathrm{V2G,ch}} \eta^{\mathrm{V2G,ch}} - P_{i,t}^{\mathrm{V2G,dis}} / \eta^{\mathrm{V2G,dis}})\Delta t + \Delta E_{i,t}^{\mathrm{V2G,change}}, \tag{2c}$$

$$\Delta E_{i,t}^{\mathrm{V2G,change}} = X_{i,t}\big(X_{i,t} - X_{i,t-1}\big) \cdot E_i^{\mathrm{V2G,arr}} - X_{i,t-1}\big(X_{i,t} - X_{i,t-1}\big) \cdot E_i^{\mathrm{V2G,dep}}, \tag{2d}$$

$$X_{i,t} \cdot E_{i,t}^{\mathrm{V2G,min}} \le E_{i,t}^{\mathrm{V2G}} \le X_{i,t} \cdot E_{i,t}^{\mathrm{V2G,max}}, \qquad \forall t \in T. \tag{2e}$$

where Eqs. (2c) are a compact form of the piece-wise equations (1c) for capturing the vehicle's charging and discharging dynamics. Particularly, the arrival and departure event $t = t_i^{\mathrm{V2G,arr}}$ and $t = t_i^{\mathrm{V2G,dep}}$ with model (1) have been encoded by $X_{i,t}\big(X_{i,t} - X_{i,t-1}\big) = 1$ and $X_{i,t-1}\big(X_{i,t} - X_{i,t-1}\big) = 1$. The term $\Delta E_{i,t}^{\mathrm{V2G,change}}$ is involved to indicate the energy variations caused by the arrival and departure event of the vehicle. Cons. (2a)-(2b) directly follow Cons. (1a)-(1b) .

The benefit of model (2) is to provide a unified representation of charging and discharging flexibility of V2Gs with heterogeneous parking duration. From the perspective of mathematics, it enables all constraints defined over the same scheduling horizon T. Moreover, each individual V2G can be viewed as a generalized virtual energy storage (VES) in the form of

$$\begin{cases} 0 \le P_{i,t}^{\mathrm{V2G,ch}} \le P_{i,t}^{\mathrm{V2G,ch,max}}, \\ 0 \le P_{i,t}^{\mathrm{V2G,dis}} \le P_{i,t}^{\mathrm{V2G,dis,max}}, \\ E_{i,t}^{\mathrm{V2G}} = E_{i,t-1}^{\mathrm{V2G}} + (P_{i,t}^{\mathrm{V2G,ch}} \eta^{\mathrm{V2G,ch}} - P_{i,t}^{\mathrm{V2G,dis}} / \eta^{\mathrm{V2G,dis}})\Delta t \\ \qquad + \Delta E_{i,t}^{\mathrm{V2G,change}}, \\ E_{i,t}^{\mathrm{V2G,min}} \le E_{i,t}^{\mathrm{V2G}} \le E_{i,t}^{\mathrm{V2G,max}}, \ \forall t \in T. \end{cases} \tag{4}$$

where the generalized VES has time-dependent power and energy capacity, and an exogenous energy change terms for capturing the arrival and departure events of the vehicle. The associated parameters are determined by the charging requirement and battery configurations of the vehicle:

$$\begin{aligned} P_{i,t}^{\mathrm{V2G,ch/dis,max}} &= X_{i,t} \cdot P_i^{\mathrm{V2G,ch/dis,max}}, \\ E_{i,t}^{\mathrm{V2G,max/min}} &= X_{i,t} \cdot E_{i,t}^{\mathrm{V2G,max/min}}, \\ \Delta E_{i,t}^{\mathrm{V2G,change}} &= X_{i,t}\big(X_{i,t} - X_{i,t-1}\big) \cdot E_i^{\mathrm{V2G,arr}} \\ &\quad - X_{i,t-1}\big(X_{i,t} - X_{i,t-1}\big) \cdot E_i^{\mathrm{V2G,dep}}, \quad \forall t \in T. \end{aligned} \tag{5}$$

Based on the generalized VES model (4), the charging and discharging flexibility of individual V2G can be represented by a 5-dimensional feature vector:

$$\begin{pmatrix} P_{i,t}^{\mathrm{V2G,agg,ch,max}}, P_{i,t}^{\mathrm{V2G,agg,dis,max}}, E_{i,t}^{\mathrm{V2G,agg,min}}, \\ E_{i,t}^{\mathrm{V2G,agg,max}}, \Delta E_{i,t}^{\mathrm{V2G,agg,change}} \end{pmatrix}, \forall t \in T. \tag{6}$$

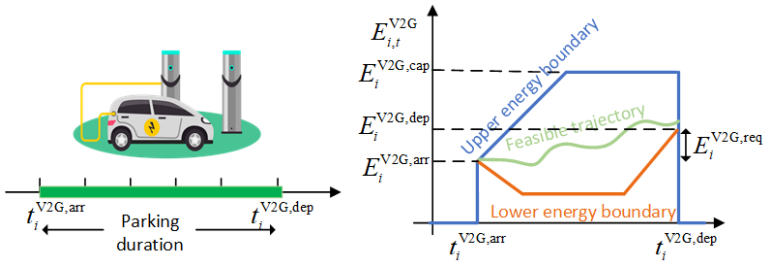

$$E_{i,t}^{\mathrm{V2G,max}} = \min\left\{ \begin{array}{l} E_i^{\mathrm{V2G,arr}} + (P_i^{\mathrm{V2G,ch,max}} \cdot (t - t_i^{\mathrm{V2G,arr}} + 1)\eta^{\mathrm{V2G,ch}})\Delta t, \\ E_i^{\mathrm{cap}} \end{array} \right\}, \quad \forall t \in T_i^{\mathrm{V2G}} \tag{3a}$$

$$E_{i,t}^{\mathrm{V2G,min}} = \max\left\{ \begin{array}{l} E_i^{\mathrm{V2G,arr}} - \left(P_i^{\mathrm{V2G,dis,max}} \cdot \left(t - t_i^{\mathrm{V2G,arr}} + 1\right) / \eta^{\mathrm{V2G,dis}}\right)\Delta t, \\ 0, \\ E_i^{\mathrm{V2G,dep}} - \left(P_i^{\mathrm{V2G,ch,max}} \cdot (t_i^{\mathrm{V2G,dep}} - t) \cdot \eta^{\mathrm{V2G,ch}}\right)\Delta t \end{array} \right\}, \quad \forall t \in T_i^{\mathrm{V2G}} \tag{3b}$$

Fig. 1. Energy envelopes for characterizing the feasible charging and discharging trajectories of individual V2G.

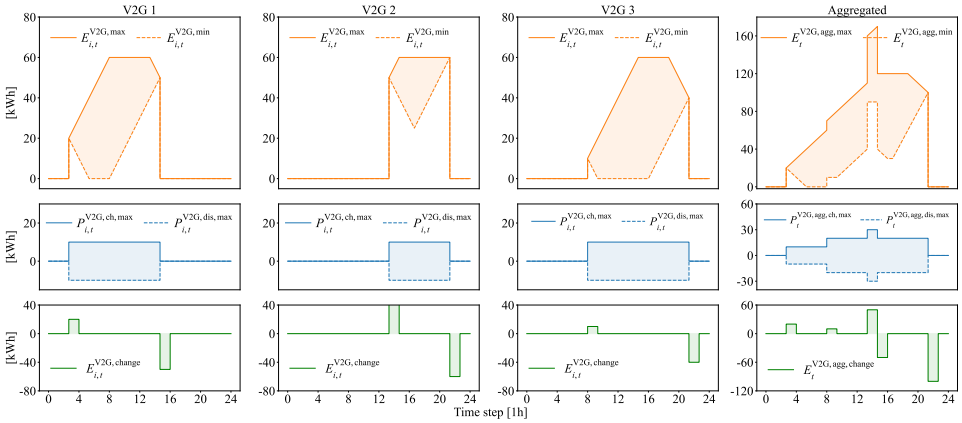

Fig. 2. An illustrative example of V2G charging and discharging flexibility characterization and aggregation

B. V2G Charging Flexibility Aggregation

The VES models (4) are additive and suitable for charging and discharging flexibility aggregation across a fleet. In fact, flexibility aggregation of V2Gs can be viewed as aggregating the small VES units of individual V2Gs into a large VES. This corresponds to aggregating the time-dependent energy and power capacity, as well as exogenous energy terms across the V2Gs fleet Ω^{V2G}:

$$\begin{aligned} P_t^{\mathrm{V2G,ch/dis,agg,max}} &= \sum\nolimits_{i\in\Omega^{\mathrm{V2G}}} P_{i,t}^{\mathrm{V2G,ch/dis,max}}, \\ E_t^{\mathrm{V2G,agg,min/max}} &= \sum\nolimits_{i\in\Omega^{\mathrm{V2G}}} E_{i,t}^{\mathrm{V2G,min/max}}, \\ \Delta E_t^{\mathrm{V2G,agg,change}} &= \sum\nolimits_{i\in\Omega^{\mathrm{V2G}}} \Delta E_{i,t}^{\mathrm{V2G,change}}, \quad \forall t \in T. \end{aligned} \tag{7}$$

This leads to the following VES model for characterizing the charging and discharging flexibility at fleet level:

$$\left\{ \begin{array}{l} 0 \le P_t^{\mathrm{V2G,agg,ch}} \le P_t^{\mathrm{V2G,agg,ch,max}}, \\ 0 \le P_t^{\mathrm{V2G,agg,dis}} \le P_t^{\mathrm{V2G,agg,dis,max}}, \\ E_t^{\mathrm{V2G,agg}} = E_{t-1}^{\mathrm{V2G,agg}} + (P_t^{\mathrm{V2G,agg,ch}} \eta^{\mathrm{V2G,ch}} - \frac{P_t^{\mathrm{V2G,agg,dis}}}{\eta^{\mathrm{V2G,dis}}})\Delta t \\ \qquad\qquad + \Delta E_t^{\mathrm{V2G,agg,change}}, \\ E_t^{\mathrm{EV,agg,min}} \le E_t^{\mathrm{EV,agg}} \le E_t^{\mathrm{EV,agg,max}}, \qquad \forall t \in T. \end{array} \right. \tag{8}$$

where $P_t^{\mathrm{V2G,ch,agg}}$, $P_t^{\mathrm{V2G,dis,agg}}$ denote the scheduled total charging and discharging power to the V2G fleet, and $E_t^{\mathrm{V2G,agg}}$ denote the aggregated energy state at the fleet level.

Based on the generalized VES model (11), the aggregated charging and discharging flexibility at the fleet level can be characterized by a similar 5-dimensional feature vector:

$$\left(\begin{array}{l} P_t^{\mathrm{V2G,agg,ch,max}}, P_t^{\mathrm{V2G,agg,dis,max}}, E_t^{\mathrm{V2G,agg,min}}, \\ E_t^{\mathrm{V2G,agg,max}}, \Delta E_t^{\mathrm{V2G,agg,change}} \end{array} \right), \forall t \in T. \tag{9}$$

Remark 1. *We have developed generalized VES models* (4) *and* (11) *to characterize the charging and discharging flexibility of individual V2Gs and V2G fleet. While model* (4) *can accurately characterize the charging and discharging flexibility of individual V2Gs, model* (4) *provides a relatively tight outer approximation of the aggregated flexibility at the fleet level. This is easy to verify as all feasible charging and discharging trajectories of individual V2Gs with model* (4) *are feasible for model* (8) *after aggregated. This paper considers obtaining an outer approximation instead of exact aggregation because computing the Minkowski sum of the heterogeneous regions characterized by model* (4) *is NP-hard. Moreover, an relatively tight approximation is generally sufficient for supporting practical applications.*

The charging and discharging flexibility characterization and aggregation for V2Gs can be interpreted from a geometric perspective. As Fig. 2 shows, the charging and discharging flexibility of each individ-

ual V2G corresponds to a 5-dimensional feature vector $(P_t^{\text{V2G,agg,ch,max}}, P_t^{\text{V2G,agg,dis,max}}, E_t^{\text{V2G,agg,min}}, E_t^{\text{V2G,agg,max}}, \Delta E_t^{\text{V2G,agg,change}}), \forall t \in T$, jointly determining the feasible region of charging and discharging trajectories of the individual V2Gs. The proposed flexibility aggregation corresponds to aggregating these small regions, yielding an extended region for characterizing the feasible charging and discharging trajectories at the fleet level.

Since unidirectional EVs can be viewed as a special case of bi-directional V2Gs with restricted discharging capability, the above results can be readily extended to EVs by setting $P_{i,t}^{\text{V2G,dis,max}} = 0$. Specifically, while following the similar notations of V2Gs, we have the following results regarding the charging flexibility characterization and aggregation for EVs.

Remark 2. *The charging flexibility of individual EVs can be characterized by the following generalized VES model:*

$$\begin{cases} 0 \le P_{i,t}^{\text{EV,ch}} \le P_{i,t}^{\text{EV,ch,max}}, \\ E_{i,t}^{\text{EV}} = E_{i,t-1}^{\text{EV}} + P_{i,t}^{\text{EV,ch}} \eta^{\text{EV,ch}} \Delta t + \Delta E_{i,t}^{\text{EV,change}}, \\ E_{i,t}^{\text{EV,min}} \le E_{i,t}^{\text{EV}} \le E_{i,t}^{\text{EV,max}}, \quad \forall t \in T, \end{cases} \tag{10}$$

associated with the following 4-dimensional feature vector:

$$\left(P_{i,t}^{\text{EV,ch,max}}, E_{i,t}^{\text{EV,min}}, E_{i,t}^{\text{EV,max}}, \Delta E_{i,t}^{\text{EV,change}}\right), \quad \forall t \in T.$$

Remark 3. *The aggregated charging flexibility of an EV fleet can be characterized by the following generalized VES model:*

$$\begin{cases} 0 \le P_t^{\text{EV,agg,ch}} \le P_t^{\text{EV,agg,ch,max}}, \\ E_t^{\text{EV,agg}} = E_{t-1}^{\text{EV,agg}} + P_t^{\text{EV,agg,ch}} \eta^{\text{EV,ch}} \Delta t + \Delta E_t^{\text{EV,agg,change}}, \\ E_t^{\text{EV,agg,min}} \le E_t^{\text{EV,agg}} \le E_t^{\text{EV,agg,max}}, \quad \forall t \in T. \end{cases} \tag{11}$$

associated with a 4-dimensional feature vector:

$$\left(P_t^{\text{EV,ch,agg,max}}, E_t^{\text{EV,agg,min}}, E_t^{\text{EV,agg,max}}, \Delta E_t^{\text{EV,agg,change}}\right), \forall t \in T. \tag{12}$$

The calculation of these feature vectors follows bi-directional V2Gs, with the discharging power capacity set to zero, i.e., $P_{i,t}^{\text{V2G,dis,max}} = 0$.

III. Physics-constrained Aggregated Charging and Discharging Flexibility Prediction

The previous section studied the characterization and aggregation of operational flexibility for bi-directional V2Gs and uni-directional EVs based on charging session data. For practical deployment, however, aggregated flexibility is required ahead of time. To this end, this section develops forecasting methods to predict aggregated flexibility from historical data. The key idea is to first derive aggregated flexibility from historical observations and then use it to forecast future flexibility.

Based on the proposed VES models, this task is formulated as a multi-variable, multi-step forecasting problem, where a multi-dimensional feature vector associated with the VES model is predicted from historical data. Specifically, we define the following vector to represent the model parameters at each time step t:

$$\boldsymbol{D}_t = \begin{cases} \begin{pmatrix} P_t^{\text{EV,ch,agg,max}}, & E_t^{\text{EV,agg,min}}, \\ E_t^{\text{EV,agg,max}}, & \Delta E_t^{\text{EV,agg,change}} \end{pmatrix}, & \text{for EV feet} \\ \begin{pmatrix} P_t^{\text{V2G,ch,agg,max}}, & P_t^{\text{V2G,dis,agg,max}}, \\ E_t^{\text{V2G,agg,min}}, & E_t^{\text{V2G,agg,max}}, \\ \Delta E_t^{\text{V2G,agg,change}} \end{pmatrix}, & \text{for V2G fleet} \end{cases} \tag{13}$$

Using historical charging data to obtain past observations, the forecasting task is formulated as

$$(\boldsymbol{D}_{t+1}, \boldsymbol{D}_{t+2}, \cdots, \boldsymbol{D}_{t+H}) = f(\boldsymbol{D}_t, \boldsymbol{D}_{t-1}, \cdots, \boldsymbol{D}_{t-K+1}, \boldsymbol{X}) \tag{14}$$

where H and K denote the prediction horizon and look-back window, respectively, $f(\cdot)$ is the forecasting model, and $\boldsymbol{X}$ includes exogenous features such as time-of-day, day-of-week, weather conditions, and the number of parked vehicles.

Although various multi-variable, multi-step forecasting methods can be applied, two main challenges arise. *First*, the energy change terms $\Delta E_t^{\text{EV,agg,change}}$ and $\Delta E_t^{\text{V2G,agg,change}}$, driven by stochastic arrivals and departures, are highly volatile and difficult to predict. *Second*, the multi-dimensional features $\boldsymbol{D}_t$ must be predicted coherently to ensure physical consistency of the feasible region (e.g., $E^{\max} \ge E^{\min}$). However, most existing methods focus on accuracy and do not explicitly enforce such consistency.

To address these challenges, we propose a physics-constrained multi-variable, multi-step forecasting framework with two key mechanisms: *(i)* structured integration of multi-dimensional features based on the VES model, and *(ii)* incorporation of physics constraints into the forecasting model to ensure coherent and physically consistent predictions.

A. A structured integration of multi-dimensional features

As introduced, the energy change terms $\Delta E_t^{\text{EV,agg,change}}$ and $\Delta E_t^{\text{V2G,agg,change}}$ with the multi-dimensional feature representation (9) and (12) induced by the random arrival and departure events of vehicles are highly volatile, posing significant challenge for the flexibility prediction. To address this challenge, we propose to reformulate the VES models to enable a structured integration of the multi-dimensional features. The core idea is to reformulate the charging and discharging dynamics with the VES model (4) to eliminate the need for a direct prediction of the energy change terms.

To achieve the objective, we revisit the aggregated charging and discharging dynamics for V2Gs:

$$\begin{aligned} E_t^{\text{V2G,agg}} = & E_{t-1}^{\text{V2G,agg}} + (P_t^{\text{V2G,agg,ch}} \eta^{\text{V2G,ch}} - \frac{P_t^{\text{V2G,agg,dis}}}{\eta^{\text{V2G,dis}}}) \Delta t \\ & + \Delta E_t^{\text{V2G,agg,change}}, \forall t \in T. \end{aligned}$$

with initial condition $E_0^{\text{V2G,agg}} = \Delta E_0^{\text{V2G,change}}$.

By unfolding the above equations across time, they can be equivalently expressed as

$$\begin{aligned} E_t^{\text{V2G,agg}} = & \sum_{\tau=0}^{t} (P_\tau^{\text{V2G,agg,ch}} \eta^{\text{V2G,ch}} - \frac{P_\tau^{\text{V2G,agg,dis}}}{\eta^{\text{V2G,dis}}}) \Delta t \\ & + \sum_{\tau=0}^{t} \Delta E_\tau^{\text{V2G,agg,change}}, \forall t \in T. \end{aligned} \tag{15}$$

By substituting (15) into the energy envelop constraints of model (8), we have

$$\begin{aligned} E_t^{\mathrm{V2G,agg,min}} - \sum_{\tau=0}^{t} \Delta E_\tau^{\mathrm{V2G,agg,change}} \\ \leq \sum_{\tau=0}^{t} (P_\tau^{\mathrm{V2G,agg,ch}} \eta^{\mathrm{EV,ch}} - \frac{P_\tau^{\mathrm{V2G,agg,dis}}}{\eta^{\mathrm{V2G,dis}}}) \Delta t \\ \leq E_t^{\mathrm{V2G,agg,max}} - \sum_{\tau=0}^{t} \Delta E_\tau^{\mathrm{V2G,agg,change}}, \quad \forall t \in T. \end{aligned}$$

By defining

$$\begin{aligned} L_t^{\mathrm{V2G,agg,min}} &= E_t^{\mathrm{V2G,agg,min}} - \sum_{\tau=0}^{t} \Delta E_\tau^{\mathrm{V2G,change}} \\ L_t^{\mathrm{V2G,agg,max}} &= E_t^{\mathrm{V2G,agg,max}} - \sum_{\tau=0}^{t} \Delta E_\tau^{\mathrm{V2G,change}} \\ L_t^{\mathrm{V2G,agg}} &= E_t^{\mathrm{V2G,agg}} - \sum_{\tau=0}^{t} \Delta E_\tau^{\mathrm{V2G,agg,change}}, \quad \forall t \in T. \end{aligned} \tag{16}$$

We have the reformulated VES model for characterizing the aggregated charging and discharging flexibility of V2Gs:

$$\begin{cases} 0 \leq P_t^{\mathrm{V2G,agg,ch}} \leq P_t^{\mathrm{V2G,agg,ch,max}}, \\ 0 \leq P_t^{\mathrm{V2G,agg,dis}} \leq P_t^{\mathrm{V2G,agg,dis,max}}, \\ L_t^{\mathrm{V2G,agg}} = L_{t-1}^{\mathrm{V2G,agg}} + (P_t^{\mathrm{V2G,agg,ch}} \eta^{\mathrm{V2G,ch}} - \frac{P_t^{\mathrm{V2G,agg,dis}}}{\eta^{\mathrm{V2G,dis}}}) \Delta t, \\ L_t^{\mathrm{V2G,agg,min}} \leq L_t^{\mathrm{EV,agg}} \leq L_t^{\mathrm{V2G,agg,max}}, \quad \forall t \in T. \end{cases} \tag{17}$$

The model is associated with a 4-dimensional feature vector:

$$\begin{pmatrix} P_t^{\mathrm{V2G,agg,ch,max}}, P_t^{\mathrm{V2G,agg,dis,max}}, \\ L_t^{\mathrm{V2G,agg,min}}, L_t^{\mathrm{V2G,agg,max}} \end{pmatrix}, \quad \forall t \in T. \tag{18}$$

The state variables $L_t^{\mathrm{V2G,agg}}$ denote the accumulative net charging of the V2G fleet up to time t. $L_t^{\mathrm{V2G,agg,min}}$ and $L_t^{\mathrm{V2G,agg,max}}$ are their lower and upper energy envelopes for capturing the charging requirements and battery operating limits. The above reformulations are readily applicable to uni-directional EVs.

It is important that the reformulated VES model (17) enables a structural integration of the multi-dimensional features with the original VES model (8). Specifically, in contrast to the original 5-dimensional feature vector (9), a 4-dimensional feature vector (18) now needs to be forecast More importantly, the resulting 4-dimensional feature vectors are much easier to forecast than the original ones due to the elimination for the direct prediction of the energy change terms. This will be clear from the numerical results.

B. Physics-constrained multi-variable and multi-step forecasting method

After reformulation, the forecasting task (14) can be adapted accordingly. The model parameters with the reformulated aggregated VES models for EVs and V2Gs at each time step t are

$$\hat{\boldsymbol{D}}_t = \begin{cases} (P_t^{\mathrm{EV,agg,ch,max}} L_t^{\mathrm{V2G,agg,min}}, L_t^{\mathrm{EV,agg,max}}), & \text{for EV fleet} \\ \begin{pmatrix} P_t^{\mathrm{V2G,agg,ch,max}}, P_t^{\mathrm{V2G,agg,dis,max}}, \\ L_t^{\mathrm{V2G,agg,min}}, \quad L_t^{\mathrm{V2G,agg,max}} \end{pmatrix}, & \text{for V2G fleet} \end{cases} \tag{19}$$

The forecasting task (14) is modified to

$$(\hat{\boldsymbol{D}}_{t+1}, \hat{\boldsymbol{D}}_{t+2}, \cdots, \hat{\boldsymbol{D}}_{t+H}) = f(\hat{\boldsymbol{D}}_t, \hat{\boldsymbol{D}}_{t-1}, \cdots, \hat{\boldsymbol{D}}_{t-K+1}, \boldsymbol{X}) \tag{20}$$

To ensure a coherent and physically consistent prediction of the multi-dimensional model parameters, we further propose a physics-constrained multi-variable and multi-step forecasting framework. As illustrated in Fig. 3, the forecasting model is composed of multi-blocks, including input block, one-step forecast blocks, H-step assemble block, physics-constrained blocks, and the output block. The input block handles the input features, including the historical observations of the model parameters $\hat{\boldsymbol{D}}_{t:t+K-1}$ and the exogenous features $\boldsymbol{X}$.

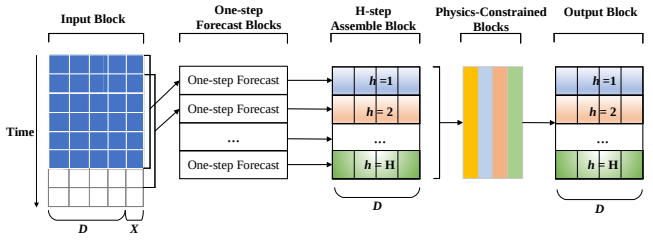

Fig. 3. Physics-constrained multi-variable and multi-step forecasting model

Following the input block is one-step forecast blocks that enable H-step forecast of the model parameters. The one-step forecast blocks handle the one-step forecasting tasks:

$$\hat{\boldsymbol{D}}_{t+h} = f\left(\hat{\boldsymbol{D}}_{t+h-H-K-1}, t \cdots, \hat{\boldsymbol{D}}_{t+h-H}, \boldsymbol{X}\right), \forall h = 1, 2, \cdots, H \tag{21}$$

where $f(\cdot)$ represents a one-step forecasting model. The H one-step forecasting tasks are performed in a parallel manner. Specifically, for each one-step forecasting task associated with the prediction step h, the model takes a sliding window of K historical observations that are H steps prior to the prediction time as input features. In particular, for the furthest prediction step $h = H$, the most recent K observations $\hat{\boldsymbol{D}}_{t-K-1:t}$ are used as inputs. It is worthy noting that the H one-step forecast blocks are designed to depend solely on historical observations and do not rely on previous predictions, which is to avoid the common accumulative prediction errors with multi-step forecasting. Besides, it is worthy noting that the proposed forecasting model represents a general forecasting framework and any existing one-step forecasting methods can be incorporated.

The subsequent H-step assemble block is responsible for stacking all one-step predictions to generate the H-step predictions $\hat{\boldsymbol{D}}_{t+1:t+H}$. Though a H-step forecast of model parameters are now available, they may not be coherent and physically consistent both temporally and spatially to ensure the feasibility of downstream optimization-oriented applications. To address this issue, physics-constrained blocks are incorporated following the H-step assemble block to ensure a cross-temporal and cross-dimensional coherent prediction. Specifically, we consider three typical physics-constrained blocks, each corresponding to a underlying principle of the aggregated model parameters. We take the bi-directional V2G as examples and the results can be readily adapted to uni-directional EVs.

1) Physics-constrained Block 1: We assume the midnight (00:00) as the initial time of each day. Since the vehicles haven't started charging and discharging, the accumulated net charged energy should be *zero* at the initial time. To enforce

this physical principle, we employ the following constraints in the forecasting model:

$$\hat{L}_t^{\mathrm{V2G,agg,min}} = 0, \quad \hat{L}_t^{\mathrm{V2G,agg,max}} = 0, \forall t = 0. \tag{22}$$

2) Physics-constrained Block 2: We have the upper energy envelopes always greater than or equal to the lower ones. To capture this characteristics, we besides involve the following constraints in the forecasting model:

$$\begin{aligned} \hat{L}_{t+h}^{\mathrm{V2G,agg,max}} &= \max\left\{\hat{L}_{t+h}^{\mathrm{V2G,agg,max}}, \hat{L}_{t+h}^{\mathrm{V2G,agg,min}}\right\}, \text{or} \\ \hat{L}_{t+h}^{\mathrm{V2G,agg,min}} &= \min\left\{\hat{L}_{t+h}^{\mathrm{V2G,agg,max}}, \hat{L}_{t+h}^{\mathrm{V2G,agg,min}}\right\}, \ \forall h \in H. \end{aligned} \tag{23}$$

3) Physics-constrained Block 3: The ramp-up and ramp-down of net energy envelopes are constrained by the maximum charging and discharging power limits of the feet. This physical principle can be captured by the following constraints:

$$\begin{aligned} \hat{L}_{t+h}^{\mathrm{V2G,agg,max}} &\leq \hat{L}_{t+h-1}^{\mathrm{V2G,agg,max}} + \hat{P}_{t+h}^{\mathrm{V2G,agg,ch,max}} \eta^{\mathrm{V2G,ch}} \Delta t, \\ \hat{L}_{t+h}^{\mathrm{EV,agg,max}} &\geq \hat{L}_{t+h-1}^{\mathrm{V2G,agg,max}} - \hat{P}_{t+h}^{\mathrm{V2G,agg,dis\,max}} / \eta^{\mathrm{V2G,dis}} \Delta t, \\ \hat{L}_{t+h}^{\mathrm{V2G,agg,min}} &\leq \hat{L}_{t+h-1}^{\mathrm{V2G,agg,min}} + \hat{P}_{t+h}^{\mathrm{V2G,agg,ch\,max}} \eta^{\mathrm{V2G,ch}} \Delta t, \\ \hat{L}_{t+h}^{\mathrm{V2G,agg,min}} &\geq \hat{L}_{t+h-1}^{\mathrm{V2G,agg,min}} - \hat{P}_{t+h}^{\mathrm{V2G,agg,ch\,max}} / \eta^{\mathrm{V2G,dis}} \Delta t, \forall h \in H. \end{aligned} \tag{24}$$

Following the physics-constrained blocks is the output block which output a H step prediction of the model parameters with the VES models, which represent the predicted aggregated charging and discharging flexibility of V2Gs.

IV. Evaluations and Applications

This section evaluates the charging and discharging flexibility characterization, aggregation and forecasting methods for bi-directional V2Gs and uni-directional EVs. Furthermore, the proposed methods are employed for the joint energy and frequency market participation of charging stations.

A. Dataset and configurations

We conduct case studies based on a real-world vehicle charging dataset that comprises 2,337 users, 2,119 charging stations, and 72,856 charging sessions collected from 2021/9/30 to 2022/9/30 [21]. Each charging session includes the detailed charging information of a vehicle, including arrival time, departure time, parking duration and required charging energy. The statistical distributions of arrival time, departure time, parking duration and charging demand are presented in Fig. 4. The average number of parked vehicles is 317.

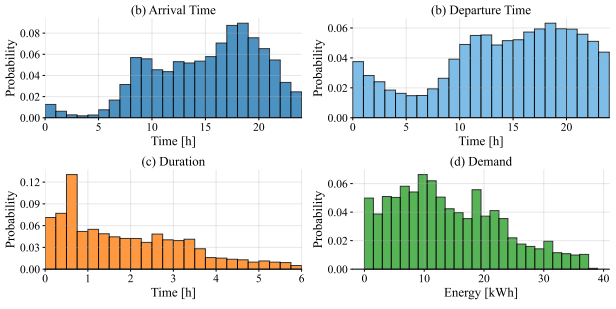

Fig. 4. Statistical distributions of the vehicle charging behaviors.

We consider two operating modes of the vehicles: uni-directional EVs and bi-directional V2Gs, and assume homogeneous battery configurations for the vehicles. Specifically, the energy and power capacity are set as 60 kWh and 5 kW, and the charging and discharging efficiency are 0.95. The dataset is in high temporal resolution and enables multi-time-scale (e.g., 5 mins, 15 mins, 30 mins, and 1 hour) characterization and aggregation of charging and discharging flexibility of vehicles.

With the charging session data, we first obtain the multi-time-scale model parameters $\{\hat{\boldsymbol{D}}_t\}$ associated with the proposed VES models, which are then used for following case studies and evaluations.

B. Effectiveness of feature integration via reformulation

This section evaluates the effectiveness of structured integration of multi-dimensional features with the VES models for prediction. Specifically, we compare the multi-dimensional features of original VES models with those of the reformulated ones. By considering all vehicles as bi-directional V2Gs, we can obtain the 5-dimensional features associated with the original VES model presented in Fig. 5. It is obvious that the energy change component $\Delta E_t^{\mathrm{V2G,agg,change}}$ is highly volatile across the time. In contrast, the resulting 4-dimensional features with the reformulated VES models show obvious cyclic characteristics and are much more amenable for forecasting as shown in Fig. 6. For uni-directional EVs, similar results can be observed as shown in Fig. 7 and Fig. 8.

While the original and reformulated VES models are mathematically equivalent, the results show that the latter are preferable in two aspects. *First*, they provide a more compact representation of the aggregated charging and discharging flexibility with reduced dimensionality of model parameters. *Second*, the model parameters of the reformulated VES models are much more amenable for forecasting.

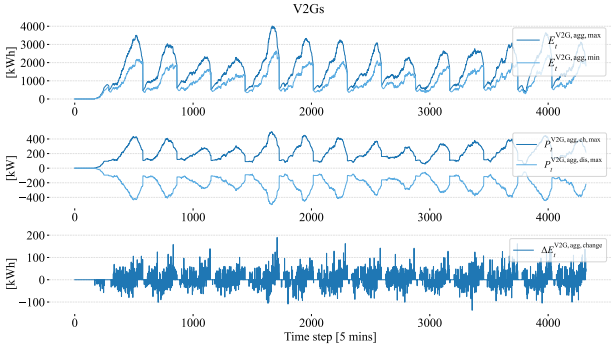

Fig. 5. Aggregated charging and discharging flexibility of V2Gs characterized by a 5-dimensional feature vector $(E_t^{\mathrm{V2G,agg,min}}, E_t^{\mathrm{V2G,agg,max}}, P_t^{\mathrm{V2G,agg,ch,max}}, P_t^{\mathrm{V2G,agg,dis,max}}, E_t^{\mathrm{V2G,agg,change}})$.

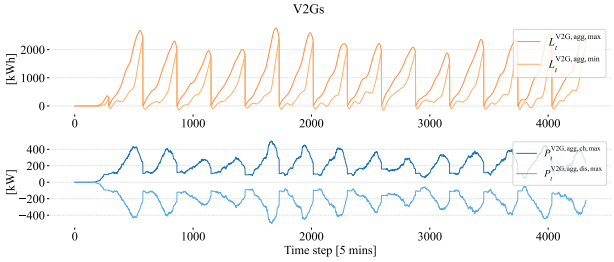

Fig. 6. Aggregated charging and discharging flexibility characterized by a 4-dimensional feature vector $(L_t^{\mathrm{V2G,agg,min}}, L_t^{\mathrm{V2G,agg,max}}, P_t^{\mathrm{V2G,agg,ch,max}}, P_t^{\mathrm{V2G,agg,dis,max}})$.

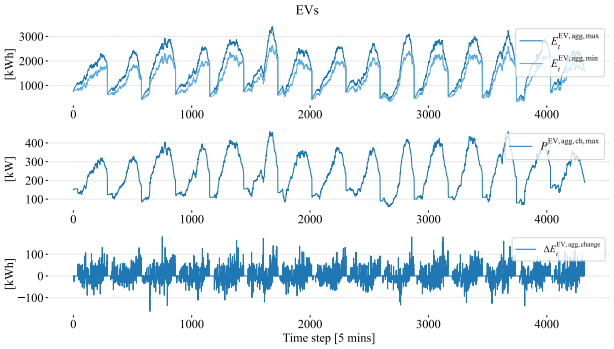

Fig. 7. Aggregated charging flexibility of EVs characterized by 4-dimensional feature vectors: $(E_t^{\mathrm{EV,agg,min}}, E_t^{\mathrm{EV,agg,max}}, P_t^{\mathrm{EV,agg,ch,max}}, E_t^{\mathrm{EV,agg,change}})$.

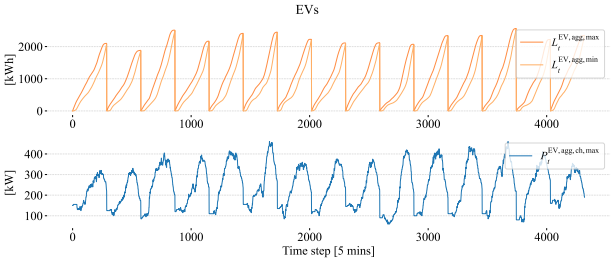

Fig. 8. Aggregated charging flexibility of EVs characterized by a 3-dimensional feature vector $(L_t^{\mathrm{EV,agg,min}}, L_t^{\mathrm{EV,agg,max}}, P_t^{\mathrm{EV,agg,ch,max}})$.

C. Aggregated charging and discharging flexibility forecasting

This section evaluates the proposed forecasting methods for multi-time-scale day-ahead predictions of aggregated vehicle charging and discharging flexibility. Without loss of generality, forecasts are generated for the next day based on historical observations. Multiple temporal resolutions (5 min, 15 min, 30 min, and 1 h) are considered. For each case, the one-year charging dataset is split into training and testing sets by a ratio of 8:2. One week of historical observations of aggregated flexibility $\hat{\boldsymbol{D}}_t$ together with the number of parked vehicles (exogenous feature $\boldsymbol{X}$) are used as model inputs. The prediction horizons and look-back windows are adjusted according to the temporal resolution (e.g., $K = 7 \times 288$, $H = 1 \times 288$ for 5-min resolution). Each dimension of input features is normalized separately. The Long Short-term Time-Series Network (**LSTNet**) model [22] and Long Short-Term Memory (**LSTM**) network are adopted as one-step forecasting blocks. We comparatively investigate the involvement of physics-constrained neural (PCNN) layers in the forecasting models. These lead to four considered methods: **LSTNet**, **LSTM**, **LSTNet + PCNN** and **LSTM + PCNN**. Widely-used performance metrics **RSE**, **MAPE**, **RMSE**, **MAE**, **CORR**, together with a user-defined geometric performance metric are used to evaluate the prediction accuracy. While the others are standard, the geometric accuracy (**ACC**) metric is defined as:

$$\mathrm{ACC} = 1 - \frac{\mathrm{Area}(\boldsymbol{Y} \setminus \hat{\boldsymbol{Y}})}{\mathrm{Area}(\boldsymbol{Y})}.$$

Where $\boldsymbol{Y}, \hat{\boldsymbol{Y}} \in \mathbb{R}^{N \times H}$ denote actual and predicted multi-dimensional VES model parameters. The ACC metric quantifies the proportion of regions of aggregated operational flexibility of vehicles captured by the predicted methods.

The performance of multi-time-scale day-ahead predictions of aggregated flexibility for V2Gs is reported in TABLE II. The ACC is evaluated by denormalized predictions, while the others are based on normalized results. We imply that all forecasting methods provide satisfactory prediction performance with Pearson Correlation Coefficient (CORR) close to 0.93 and ACC close to 0.86. In addition, the coherence and physical consistency of the predicted multi-dimensional VES model parameters are also evaluated by examining the satisfaction of physical constraints in (22)-(24). The results show that almost all day-ahead predictions violate some of the consistency constraints when the PCNN layers are absent. In contrast, the coherency and physical coherence indicated by the constraints (22)-(24) can be provided by the PCNN-enhanced methods. Besides, it is worth noting that the involvement of PCNN layers does not obviously affecting the prediction accuracy.

In addition to prediction performance, training time of all forecasting methods is also evaluated and reported in TABLE II. The results show that the training time shows an increasing trend with finer temporal resolutions. This trend is particularly obvious with the LSTNet method. This is because a forecasting task with a finer temporal resolution relies on relatively larger forecasting models. Besides, the results show that incorporating the PCNN layers will slightly increase the training time but not that obvious. For uni-directional EVs, similar results are available from TABLE III.

We further investigate the prediction performance from a geometric perspective. Due to space limits, we only display the results of **LSTNet + PCNN** method at a temporal resolution of 30 mins. The actual and predicted feasible regions for aggregated flexibility of V2Gs for 10 testing days are presented in Fig. 9. It is worth noting that the boundaries directly correspond to the 4-dimensional model parameters associated with the reformulated VES models. The actual and predicted feasible regions are distinguished by different transparencies. Since the two areas align well, we conclude that the proposed forecasting methods are able to well capture the aggregated charging and discharging flexibility of vehicles. Similar results can be observed with EVs as shown in Fig. 10. The major difference is that EVs exhibit slightly reduced operational flexibility as they can only get charged during parking durations.

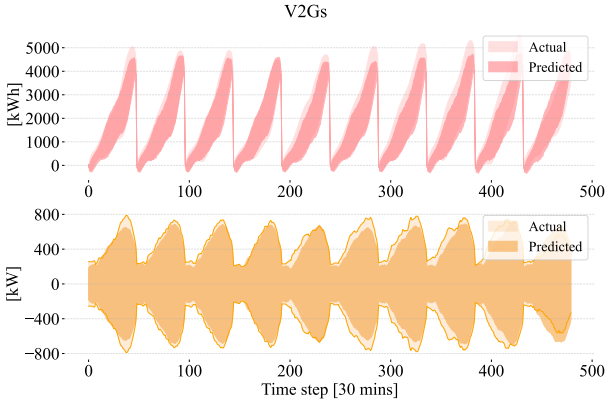

Fig. 9. Actual and predicted of charging and discharging for V2G fleet with LSTNet + PCNN method for 10 testing days

D. Joint participation in energy and frequency markets

This section evaluates the proposed flexibility characterization, aggregation, and forecasting framework for the joint energy and frequency market participation of charging stations.

TABLE II
MULTI-TIME-SCALE DAY-AHEAD PREDICTION OF AGGREGATED CHARGING AND DISCHARGING FLEXIBILITY FOR V2GS.

Forecast Models	Temporal Resolutions	RSE	MAPE	RMSE	MAE	CORR	ACC	Training Time[s]	Coherence
LSTNet	1h	0.3270	0.2535	0.0865	0.0537	0.9452	0.8744	0.92	0%
	30min	0.3319	0.2495	0.0867	0.0556	0.9444	0.8611	1.20	0%
	15min	0.3327	0.2421	0.0863	0.0550	0.9441	0.8597	2.48	0%
	5min	0.3446	0.2608	0.0888	0.0582	0.9400	0.8458	11.84	0%
LSTM	1h	0.3539	0.2663	0.0935	0.0621	0.9395	0.8381	0.06	0%
	30min	0.3626	0.2651	0.0947	0.0612	0.9329	0.8518	0.08	0%
	15min	0.3657	0.2673	0.0612	0.0612	0.9309	0.8367	0.12	0%
	5min	0.3750	0.2710	0.0622	0.0622	0.9271	0.8521	0.29	0%
LSTNet + PCNN	1h	0.3417	0.2470	0.0904	0.0584	0.9408	0.8462	6.79	100%
	30min	0.3374	0.2494	0.0881	0.0568	0.9426	0.8560	13.31	100%
	15min	0.3529	0.2413	0.0915	0.0602	0.9406	0.8295	26.13	100%
	5min	0.3585	0.2725	0.0924	0.0612	0.9348	0.8398	81.80	100%
LSTM + PCNN	1h	0.3603	0.2470	0.0952	0.0623	0.9367	0.8375	0.23	100%
	30min	0.3688	0.2719	0.0963	0.0644	0.9316	0.8268	0.46	100%
	15min	0.3672	0.2686	0.0951	0.0617	0.9304	0.8541	0.91	100%
	5min	0.3693	0.2858	0.0951	0.0611	0.9300	0.8829	2.66	100%

TABLE III
MULTI-TIME-SCALE DAY-AHEAD PREDICTION OF AGGREGATED CHARGING AND DISCHARGING FLEXIBILITY FOR EVS

Forecast Models	Temporal Resolutions	RSE	MAPE	RMSE	MAE	CORR	ACC	Training Time[s]	Feasibility
LSTNet	1h	0.3444	0.2218	0.0877	0.0544	0.9390	0.8609	0.92	0%
	30min	0.3547	0.2384	0.0891	0.0576	0.9356	0.8416	1.21	0%
	15min	0.3625	0.2296	0.0905	0.0601	0.9369	0.8143	2.48	0%
	5min	0.3778	0.2367	0.0938	0.0620	0.9274	0.8192	11.48	0%
LSTM	1h	0.3756	0.2355	0.0955	0.0634	0.9318	0.8160	0.06	0%
	30min	0.3824	0.2370	0.0960	0.0620	0.9243	0.8493	0.08	0%
	15min	0.3861	0.2360	0.0963	0.0622	0.9227	0.8368	0.12	0%
	5min	0.3966	0.2431	0.0984	0.0635	0.9181	0.8471	0.29	0%
LSTNet + PCNN	1h	0.2690	0.2064	0.0915	0.0584	0.9342	0.8329	6.20	100%
	30min	0.2811	0.2219	0.0930	0.0602	0.9310	0.8164	12.39	100%
	15min	0.3130	0.2329	0.0990	0.0667	0.9243	0.7918	22.90	100%
	5min	0.2894	0.2367	0.0929	0.0614	0.9289	0.8294	67.15	100%
LSTM + PCNN	1h	0.3846	0.2222	0.0978	0.0643	0.9294	0.8047	0.22	100%
	30min	0.3831	0.2395	0.0986	0.0657	0.9216	0.8036	0.36	100%
	15min	0.3882	0.2380	0.0968	0.0629	0.9217	0.8298	0.71	100%
	5min	0.3910	0.2444	0.0970	0.0625	0.9208	0.8319	2.12	100%

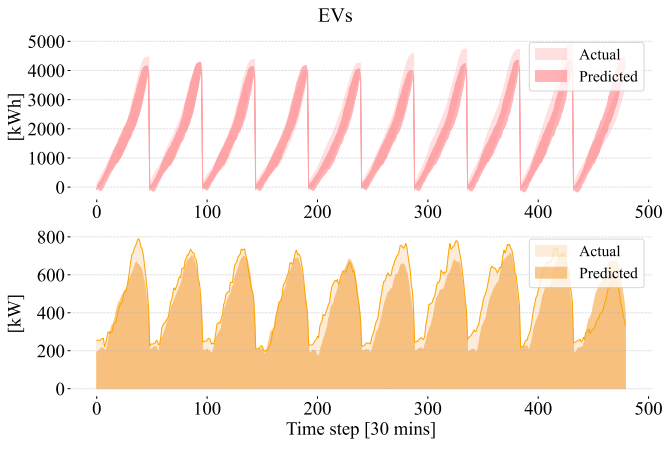

Fig. 10. Actual and predicted feasible region of charging for EV fleet with LSTNet + PCNN method for 10 testing days

We consider a charging station providing charging services to EVs and V2Gs, and meanwhile participating in energy and frequency markets by leveraging vehicle flexibility to gain economic benefits. The PJM electricity markets, including day-ahead energy, real-time energy, and frequency markets, are considered. The day-ahead markets operate hourly, while the real-time market clears every 5 minutes. Historical market clearing prices are obtained from the PJM official website [23]. For market participation, the charging station needs to submit day-ahead bids (energy and capacity) for all trading intervals of the following day. As day-ahead bidding depends on vehicle flexibility, the trained LSTNet + PCNN model is used to obtain day-ahead predictions of aggregated flexibility at a temporal resolution of 5 mins, which serves as constraints of a multi-stage bidding optimization problem. Three case studies that involve EVs, V2Gs or their combinations are considered. For joint participation, bidding strategies are co-optimized to maximize economic benefits.

We evaluate both the effects of aggregation and prediction for market participation of charging stations. We consider three settings for each case study: **Individual w/o prediction**, **Aggregated w/o prediction** and **Aggregated with prediction**. For Individual w/o prediction, we compute the daily optimal bidding strategies based on the individual vehicle models without any aggregation. For Aggregated w/o prediction, we compute the optimal bidding strategies based on the actual aggregated flexibility. For the last Aggregated with prediction,

we compute the optimal bidding strategies based on the day-ahead predicted aggregated flexibility. It is worth noting that complete information regarding the charging and discharging flexibility of vehicles is assumed for the first two settings. The Individual w/o prediction method provides the theoretical optima and can be used to evaluate the performance gaps caused by aggregation and prediction.

All case studies are conducted on 30-day dataset. While the bidding strategies for energy and frequency markets are optimized jointly, the *ex-post* market profits are evaluated separately to give more details. TABLE IV presents the results of three cases under the three settings. The average daily profit and average solving time to obtain the optimal bidding strategies are used as the performance metrics. The gap of market profit is evaluated by the theoretical optimum provided by Individual w/o prediction. We observe that the **Aggregated w/o prediction** method leads to slight overestimation of average daily market profit by 0.58-4.78% across the case studies. This actually indicates the loss of outer approximation of aggregated flexibility with the proposed aggregation method. Further, by comparing **Aggregated with prediction** and **Individual w/o prediction**, we find that the performance gaps caused by both aggregation loss and prediction error are about 3.0-9.4%. Notably, this gap is mitigated due to the opposite effects of aggregation and prediction.While aggregation tends to overestimate the operational flexibility due to its outer approximation nature, the forecasting methods tend to generate underestimated predictions. The performance gaps are acceptable considering the substantially improved computational efficiency. Specifically, the average computation time for obtaining optimal bidding strategies is reduced from 10-22 mins to seconds through aggregation.

The effectiveness of the proposed aggregation and forecasting methods for supporting the market participation of charging station is further illustrated in Fig. 11-12, which present the obtained bidding strategies for joint energy markets for three test days of Case 3. The results show that the bidding strategies obtained from the aggregated and forecasting models are quite close to the theoretical optima.

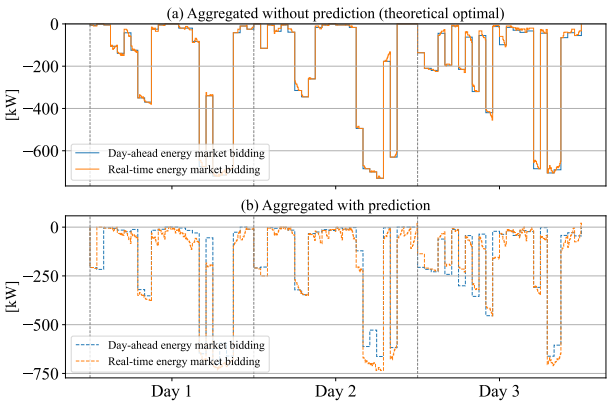

Fig. 11. Bidding strategies of charging station in day-ahead and real-time energy market with Case 3 for three testing days

V. Conclusion

This paper investigated the charging and discharging flexibility characterization, aggregation and forecasting methods

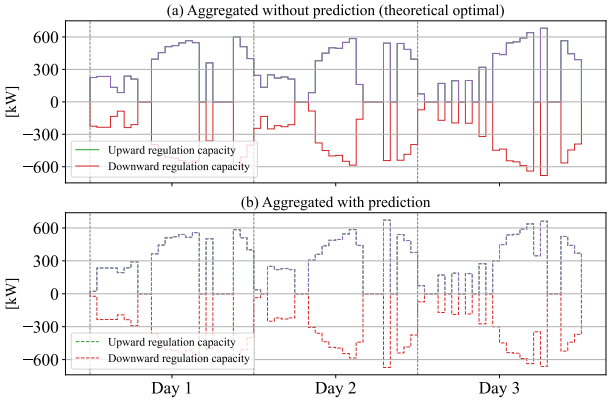

Fig. 12. Bidding strategies of charging station in day-ahead frequency market with Case 3 for three testing days

for bi-directional V2Gs and uni-directional EVs. A generalized virtual energy storage (VES) model was proposed to effectively characterize the charging and discharging flexibility both at the vehicle and fleet level. We further proposed a physics-constrained forecasting method to predict the aggregated flexibility at fleet level from historical charging session data under uncertainty. The effectiveness of proposed methods were evaluated using real-word vehicle charging datasets and validated for the joint energy and frequency market participation of charging stations. Results show that the proposed forecasting method enables multi-time-scale day-ahead predictions of aggregated operational flexibility of EVs and V2Gs at a prediction accuracy close to 86% and the Pearson correlation coefficient (CORR) close to 0.93. For the joint market participation, the performance gap caused by aggregation is less than 5%, and the combined loss caused by both aggregation and prediction remains below 10%. Whereas, the computational efficiency of obtaining the optimal bidding strategies of charging stations was significantly improved from 10-20 mins to second levels through aggregation.

References

[1] International Energy Agency, “Global EV Outlook 2025,” 2025. Available: https://www.iea.org/reports/global-ev-outlook-2025.

[2] Department for Transport, UK Government, “Phasing out sales of new petrol and diesel cars from 2030 and supporting the zero emission transition,” 2025. Available: https://assets.publishing.service.gov.uk/media/679382182de28ea2d392f37f/phasing-out-the-sale-of-new-petrol-and-diesel-cars-from-2030-and-support-for-the-zero-emission-transition.pdf.

[3] F. Ahmed, S. Ahmad, M. T. Rahman, M. R. Hazari, R. Faiz, T. Ahmed, and M. Karimi, “A holistic review of electric vehicle charging impacts on power distribution networks: Technical challenges, smart mitigation strategies and future directions,” *Applied Energy*, vol. 402, p. 126961, 2026.

[4] A. R. Singh, R. S. Kumar, K. R. Madhavi, F. Alsaif, M. Bajaj, and I. Zaitsev, “Optimizing demand response and load balancing in smart ev charging networks using ai integrated blockchain framework,” *Scientific Reports*, vol. 14, no. 1, p. 31768, 2024.

[5] Z. Kang, Z. Ye, C.-M. Lam, and S.-C. Hsu, “Sustainable electric vehicle charging coordination: Balancing co2 emission reduction and peak power demand shaving,” *Applied Energy*, vol. 349, p. 121637, 2023.

[6] B. Xu, W. Luan, B. Zhao, and C. Long, “Frequency regulation provision by ev aggregator with dynamic balance between user

TABLE IV
MARKET OUTCOMES OF CHARGING STATION PARTICIPATION IN ENERGY AND FREQUENCY MARKETS

Case	**Market**	**Individual w/o prediction**		**Aggregated w/o prediction**			**Aggregated with prediction**		
		Profit [$]	Time [s]	Profit [$]	Time [s]	Gap [%]	Profit [$]	Time [s]	Gap [%]
Case 1: EVs	Energy	-1275.86	46.31	-1256.78	0.03	+1.50	-1381.19	0.02	-8.25
	Frequency	1837.08		1895.06		+3.16	1730.07		-5.83
Case 2: V2Gs	Energy	-1178.46	724.39	-1163.54	0.31	+1.27	-1275.41	0.29	-8.23
	Frequency	3181.56		3333.51		+4.78	3068.69		-3.55
Case 3: EVs + V2Gs	Energy	-2452.54	1321.29	-2438.31	0.68	+0.58	-2683.15	0.75	-9.40
	Frequency	4631.83		4833.85		+4.36	4492.55		-3.01

charging anxiety and aggregate flexibility," *IEEE Transactions on Smart Grid*, 2025.

[7] M. Pertl, F. Carducci, M. Tabone, M. Marinelli, S. Kiliccote, and E. C. Kara, "An equivalent time-variant storage model to harness ev flexibility: Forecast and aggregation," *IEEE transactions on industrial informatics*, vol. 15, no. 4, pp. 1899–1910, 2018.

[8] H. Zhang, Z. Hu, Z. Xu, and Y. Song, "Evaluation of achievable vehicle-to-grid capacity using aggregate pev model," *IEEE Transactions on Power Systems*, vol. 32, no. 1, pp. 784–794, 2016.

[9] Z. Yi, D. Scoffield, J. Smart, A. Meintz, M. Jun, M. Mohanpurkar, and A. Medam, "A highly efficient control framework for centralized residential charging coordination of large electric vehicle populations," *International Journal of Electrical Power & Energy Systems*, vol. 117, p. 105661, 2020.

[10] D. Yan, C. Ma, and Y. Chen, "Distributed coordination of charging stations considering aggregate ev power flexibility," *IEEE Transactions on Sustainable Energy*, vol. 14, no. 1, pp. 356–370, 2022.

[11] F. L. Müller, J. Szabó, O. Sundström, and J. Lygeros, "Aggregation and disaggregation of energetic flexibility from distributed energy resources," *IEEE Transactions on Smart Grid*, vol. 10, no. 2, pp. 1205–1214, 2017.

[12] F. Al Taha, T. Vincent, and E. Bitar, "An efficient method for quantifying the aggregate flexibility of plug-in electric vehicle populations," *IEEE Transactions on Smart Grid*, 2024.

[13] Y. Wen, Z. Hu, S. You, and X. Duan, "Aggregate feasible region of ders: Exact formulation and approximate models," *IEEE Transactions on Smart Grid*, vol. 13, no. 6, pp. 4405–4423, 2022.

[14] S. Taheri, V. Kekatos, S. Veeramachaneni, and B. Zhang, "Data-driven modeling of aggregate flexibility under uncertain and non-convex device models," *IEEE Transactions on Smart Grid*, vol. 13, no. 6, pp. 4572–4582, 2022.

[15] M. Jenkins and I. Kockar, "Electric vehicle aggregation model: A probabilistic approach in representing flexibility," *Electric Power Systems Research*, vol. 213, p. 108484, 2022.

[16] E. Genov, C. De Cauwer, G. Van Kriekinge, T. Coosemans, and M. Messagie, "Forecasting flexibility of charging of electric vehicles: Tree and cluster-based methods," *Applied Energy*, vol. 353, p. 121969, 2024.

[17] M. Zhang, Y. Xu, X. Shi, and Q. Guo, "A fast polytope-based approach for aggregating large-scale electric vehicles in the joint market under uncertainty," *IEEE Transactions on Smart Grid*, vol. 15, no. 1, pp. 701–713, 2023.

[18] K. Mukhi, C. Qu, P. You, and A. Abate, "Robust aggregation of electric vehicle flexibility," in *Proceedings of the 28th ACM International Conference on Hybrid Systems: Computation and Control*, pp. 1–10, 2025.

[19] N. Brinkel, L. Visser, W. van Sark, and T. AlSkaif, "A novel forecasting approach to schedule aggregated electric vehicle charging," *Energy and AI*, vol. 14, p. 100297, 2023.

[20] Z. Chen and Z. Hu, "Evaluating and forecasting the aggregate flexibility of large-scale electric vehicle charging and swapping facilities," *IEEE Transactions on Transportation Electrification*, 2026.

[21] K. Baek, E. Lee, and J. Kim, "A dataset for multi-faceted analysis of electric vehicle charging transactions," *Scientific Data*, vol. 11, no. 1, p. 262, 2024.

[22] G. Lai, W.-C. Chang, Y. Yang, and H. Liu, "Modeling long- and short-term temporal patterns with deep neural networks," in *The 41st international ACM SIGIR conference on research & development in information retrieval*, pp. 95–104, 2018.

[23] PJM Interconnection, "Daily Energy Market Offer Data," 2026. Available: https://www.pjm.com/markets-and-operations/energy/real-time/historical-bid-data/unit-bid.aspx.